Journal of Materials Chemistry B

Accepted Manuscript

ROYAL SOCIETY OF CHEMISTRY

www.rsc.org/materialsB

Tellurium Platinate Nanowires for Photothermal therapy of Cancer cells

Sunil Pandey[1, 5] Abou Talib[4], M. Mukeshchand Thakur[6], M. Shahnawaz Khan[4,] Mukesh Lavkush Bhaisare[1], Gangaraju Gedda[4], Hui-Fen Wu*[1, 2, 3, 4, 5]

[1]Department of Chemistry, National Sun Yat-Sen University, Kaohsiung, 70, Lien-Hai Road, Kaohsiung, 80424, Taiwan

[2] School of Pharmacy, College of Pharmacy, Kaohsiung Medical University, Kaohsiung, 807, Taiwan

[3]Institute of Medical Science and Technology, National Sun Yat-Sen University, 80424, Taiwan

[4] Doctoral Degree Program in Marine Biotechnology, National Sun Yat-Sen University and Academia Sinica, Kaohsiung, 80424, Taiwan

[5]Center for Nanoscience and Nanotechnology, National Sun Yat-Sen University, 70, Lien-Hai Road, Kaohsiung, 80424, Taiwan

[6]School of Biotechnology and Bioinformatics, D.Y. Patil University, CBD-Belapur, Navi Mumbai- 400 614, Maharashtra, India

***Corresponding author, Phone: +886-7-5252000-3955; Fax: +886-7-5253908**

Email: hwu@faculty.nsysu.edu.tw

Abstract

Among the most celebrated modes of cancer treatment, photothermal therapy is the most potential tools over past few years. In spite of surplus introduction of novel nanomaterials for photothermal therapy, there is still plenty of chance for exploration of naïve materials. We have explored the photothermal properties of metal chalcogenides called Tellurium Platinate nanowires (TePt NWrs) in this work. Upon irradiation with the laser (Ti: sapphire laser, 808nm) the temperature of aqueous suspension of TePt NS was found to rise to ~62°C from room temperature at optimum concentrations. This was due to stability and high photothermal transduction efficiency of nano-rods (NRs) i.e. ~47 %. The power to ablate tumor cells was studied using A549 cells and tumor grafted experimental mice models. After an initial exposure of 10 min (808 nm laser at 1 W/cm^2), the cells were killed mainly by the process of apoptosis as confirmed by Flow cytometry assisted cell sorting system (FACS; PI-FITC-Annexin V staining). Tumor growth was significantly reduced after the photothermal therapy via the combination of the TePt NRs and laser; thus proving the important evidence for this new nanomaterial for cancer photothermal therapy. The current approach has introduced a highly potential photothermal therapy method for medical world in the near future.

Keywords: Tellurium Platinate, Photothermal therapy, Photothermal transduction efficiency, A549 cells, in vivo

1. Introduction

Due to physico-anatomical alterations of tumor microenvironment, the entry of drugs and other essential metabolites becomes difficult task leading to development of drug resistance and other molecular complications in cancer chemotherapy[1]. The strategies to enhance the one to one interaction of the chemotherapeutic agents with the target can unravel novel platforms to combat with rapid progression of cancerous cells and metastatic transformations[2]. The distortions in tumor anatomy and poor fluid perfusion[3,4], high extracellular matrix densities in the tumor microenvironment[5], severely compromised lymphatic drainage and high interstial fluid pressure[6] and non-specific weak interactions with extracellular components are the most cardinal issues for cancer chemotherapy.

In past few years, the combinatorial therapies have emerged as promising alternatives to existing drug delivery strategies[7]. Photothermal therapy (PTT) and photodynamic therapy (PDT) has snatched the special consideration to be used as a potential therapy for solid tumors[8]. These two techniques can be combined with chemotherapy to enhance the permeability and retention of the drugs inside the solid tumors[3]. In a stark contrast to surgical and radiological techniques, PTT and PDT are minimal invasive techniques and require less expenditure[9,10]. PTT, which employs heat above 43°C, enhances the vascular permeability for several folds, thus enabling the interaction of chemotherapeutic agents with the targets. The hyperthermia enhances the blood flow and extravasations of macromolecules. The resulting pressure and cytoskeleton damage leads to cell death[3]. PDT is an alternative, which is considered to be safer than PTT in many ways. When the temperature shoots above 43°C, many sensitive tissue such as intestinal gut lines become damaged leading to some adverse side effects (Song 1984). Typically, PDT exploits the capacity to produce free radicals or other toxic chemical moieties, which kill cancer cells selectively.

Recently, many nanoparticles (have been investigated for photothermal killing of cancer cells such as pleomorphic gold NPs[11-14], plasmonic semiconductor NPs[15], DNA anchored NPs[16], platinum NPs[17], and Carbon quantum dots modified gold NRs[18]. Some recent efforts used metal nano-composite such as such as CuTe, CuS and CuSe for photothermal ablation of cancer cells[19]. Crystalline form of metal chalcogenides due to their magnificent size dependent properties, have been exploited in variety of novel application including Surface Enhanced Raman Spectroscopy (SERS)[20-22]. Among transition metals chalcogenides, tellurium based compounds have been widely explored for many novel applications such as solar cells, photovoltaic, optical, thermo-electronics and biological labeling[23-33]. One of the finest examples of metal chalcogenides is the TePt-based NPs. They form an excellent combination of metal and semiconductor moieties making them to be ideal as binary nano-systems[34-36] for photothermal therapy of cancer cells. Present protocol for the synthesis of synthesis of TePt is a slight departure from the earlier template assisted method to make 1D TePt[37] . We have made an attempt to develop one pot synthesis at 200°C in the presence of hydrazine, platinum hexachloride ($PtCl_6$) and Cetyltriammonium bromide (CTAB) to confer positive charges in order to facilitate their interaction with biological cells.

In the present work, we have tuned the synthesis of TePt NWrs for the photothermal therapy. A detailed investigation of photothermal property of the proposed NPs along with in vivo studied on experimental mice models is carefully conducted. The photothermal conversion efficiency of the TePt NWrs was found to very high at a particular concentration. In vivo infrared thermal imaging experiments demonstrated the enhancement of temperature above 50°C using NIR laser (λ=808nm). The mode of killing was confirmed by staining the post irradiated A549 cells by PI-FITC-Annexin V staining and analyzing using FACS system.

2. Experimental

2.1 Materials

Hydrazine, $PtCl_6$, CTAB, and Tellurium dioxide (TeO_2) were purchased form Sigma, USA and used as received without further purification. Lysozyme was purchased from Fluka, UK. Neutral red dye, 2, 5-diphenyl-3-(4, 5-dimethyl-2-thiozyl) tetrazolium bromide (MTT), dimethyl sulfoxide (DMSO) were purchased from Sigma-Aldrich (St. Louis, MO, USA). A549 cells were purchased from Bioresource Collection and Research Center (BCRC), Taiwan and cultured as per the instructions provided by the company. Dulbecco's modified Eagle's medium was purchased from Thermo Scientific, USA (DMEM, HyClone® containing 4mM/l L-glutamine, 4500 mg/l glucose) fetal bovine serum (FBS) were purchased from Gibco, USA. Phosphate buffer saline (PBS), trypsin-EDTA solution (17,000 U/l trypsin mixed with 0.2g/l EDTA) and pen-strep solution (10000 U/ml penicillin mixed with 10 mg/ml streptomycin) and trypan blue were obtained from Lonza, Belgium.

2.2 Methods

2.2.1 Synthesis of TePt nanoparticles

The TePt NWrs were synthesized using modified template-assisted method using CTAB. The tellurium nanowires were synthesized by adding 5 ml hydrazine to solution containing 8 mg of TeO_2 under mild stirring (1.5-2h) till the solution turned to deep blue color to confirm the formation of tellurium nanowires. This solution was centrifuged and dialyzed against pure water for 12 h. This purified precipitate was mixed with solution containing 10 mM CTAB and allowed to disperse for 20 min. Next, 1.5 ml of 10 mM $PtCl_6$ was added to this solution under stirring and sealed in Teflon coated container. The container was kept at 100˚C for 12 h to synthesize the TePt NWrs. Maximum amount of CTAB was removed by washing the mixture with water followed by dialysis against distilled water for 24 h.

2.2.2 Characterization

The morphological details of TePt NWrs were elucidated using transmission electron microscope (TEM) (Philips, The Nederlands). UV-Vis-NIR spectroscopy (Thermo Evolution 201, USA) was carried out using standard quartz cuvette having path length 1 cm. 2 µl of the samples were drop coated on formwar coated copper grids to form uniform layer and dried under ambient temperature to ensure the integrity of the film. Crystallographic details of NPs were studied using powder X-ray diffraction (XRD, Phillips, The Nederlands).

2.2.3 In vitro photothermal efficiency of TePt NWrs

In order to check the photothermal performance of TePt NWrs different amount ranging from 1-10 µg ml^{-1} (0.5 ml total volume) was taken in mini-quartz cuvette and irradiated with 808 nm laser for 10 min. The power density of laser was adjusted to 1 W/cm^2. The enhancement in the temperature was recorded using thermal imaging camera (FLIR E8, Sweden). In order to scrutinize the photo-stability of the TePt NWrs, ten microgram of the aqueous suspension of NPs was irradiated with laser for 10 min (ON) followed by natural cooling of the nanoparticle suspension after switching off the laser (OFF). This ON-OFF cycle was repeated 10 times in order to validate the claim.

2.2.4 Routine maintenance of cell line and cytotoxicity of NPs

Lung carcinoma (A549) cells were seeded at a density of 3 x 10^4 cells/well in a 96 well-plate cultured in DMEM medium (8.5 % fetal bovine serum and 0.5 % penicillin-streptomycin mixture) at the standard conditions of 5% CO_2 at 37°C. For evaluating cytotoxicity, MTT-based assay was done as per previous studies and cytotoxicity was measured spectrophotometrically at 570 nm after 24 h. In another approach, Trypan blue dye-exclusion assay was used to analyses cell viability. Controls used were, only cells and untreated cells with laser alone. The similar

procedure was repeated after irradiation of laser to TePt NWrs with A549 cells in different concentrations as presented in the Figure 4.

2.2.5 In vivo photothermal studies

Healthy ICR mice (Lasco, Charles River Technology, Taiwan) weighing 18-20 g were used for comprehending the photothermal ability of the NPs under tumor microenvironment. The experimental protocol involving animal model review committee approved by NSYSU, Animal and use committee, 2015-16. The Animals were handled under the ethical guidelines provided by the above committee. Induction of the tumor in mice was done as per the previous methods. Briefly, A549 cells (300µl of $2x10^8$ cells/ml in Hanks balanced salt solution) were injected in the right flank of the mice. The mice were considered for experimentation after the growth of the tumors was ensured to 100-150 mm in diameter. The mice were anaesthetized using standard procedures. In order to check the in vivo photothermal property of TePt NWrs, nearly 100 µl of purified TePt NWrs in PBS was injected intra-tumorally using hypodermic needle. The control mice were injected with PBS alone. TePt NWrs were allowed to disperse inside the tumor for nearly 1.5 h. The tumor surface was irradiated with laser for 10 min. The raise in the temperature was recorded using thermal imaging camera (FLIR, Sweden). To assess the post-irradiation internal anatomy tumor, the mice were euthanized and the tumor was removed to make wax embedded cake of treated tumor. Thin sections were made using microtomy and stained using hematoxylin/eosin (H&E). The slices were observed under inverted microscopy. The volume of the post-treated tumors was calculated (with respect to control) using following equation:

$$Tumorvolume = \left(Length \times Width^2 \Big/ 2 \right) \qquad (1)$$

2.2.6 Analysis of the cells death after photothermal therapy

Post laser irradiated A549 cells in presence of TePt NWrs were stained with FITC-Annexin V and PI to understand the mode of killing. The staining was done as per the instructions provided by the manufacture (Strong Biotech Corporation, Taiwan). In short, actively growing A549 cells

(~10^7 cells/ml) treted with laser in presence of NPs. For the FACS analysis, cells were stained with 2µl of FITC-Annexin V and PI were (mixed with 100µl of the binding buffer) and incubated in dark for 20 min. The samples were analysed by flow cytometry (CyflowSL, Partec Germany) equipped with 488 nm solid-state laser.

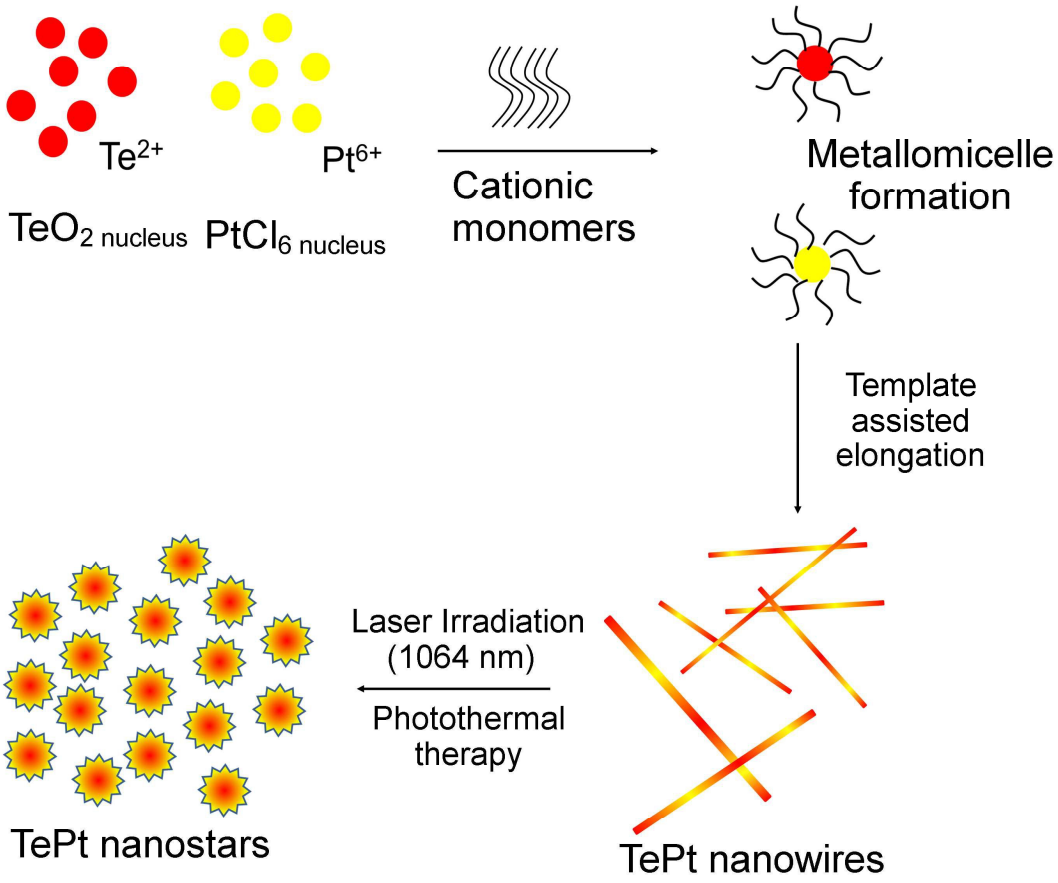

Figure 1. Schematic representation showing scheme of synthesis of TePt nano-wires and nanostars/nanoparticles.

3. Results and discussion

Figure 1 shows the schematic representation of the synthesis process at a glance. Tellurium NWRs were synthesized in presence of hydrazine, which was further allowed to react with platinum ions in presence of CTAB to yield TePt NWrs. The concentration of CTAB was

187 adjusted above critical micelle concentration. As per some earlier theories about the intricate
188 relationship between the shape and photothermal properties of nanomaterial, the hyper-branched
189 and spiny structures are most suitable for photo-thermal assassination of cancer cells[38] (Liu et al.
190 2014).

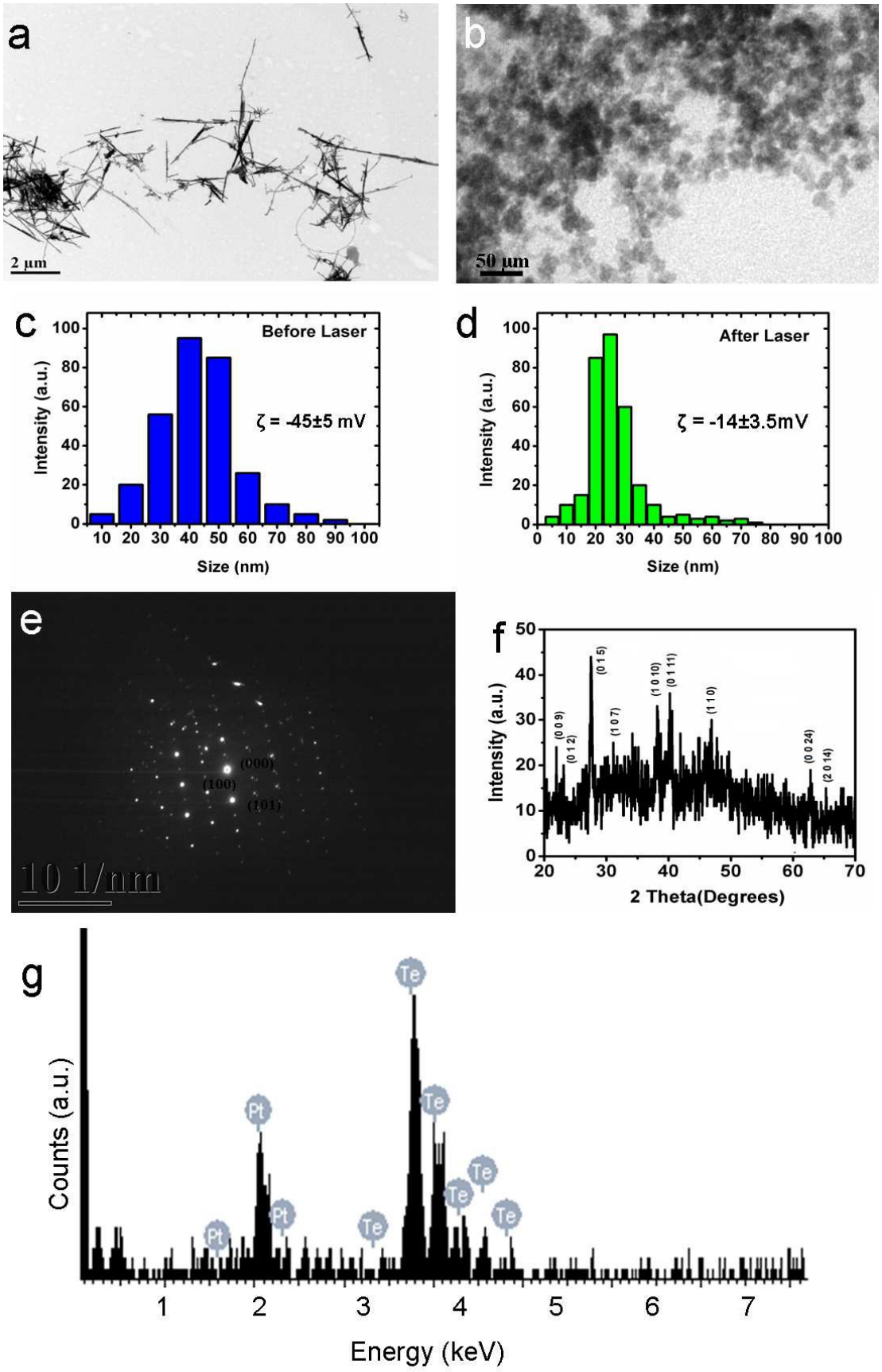

Figure 2. The morphological and physical properties of TePt NWrs (a) before exposure of laser (1064 nm), (b) image of the same after exposure to laser, size analysis, (c) before and (d) after laser treatment using DLS and inset zeta values are represented as mean±SD, (e) SAED pattern of TePt NS exhibiting crystalline nature, (f) XRD, and (g) EDAX spectra showing the elemental composition.

Fi Figure 2 a represents the TEM of TePt NWrs synthesized using hydrazine. The size of TePt NWrs was found to be ~10 μm. After irradiation with laser, TePt NWrs got transformed to TePt nanostars ranging from 20-30 nm in size (Fig.2b). Fig. 2 c-d shows DLS analysis with zeta value more stable before laser irradiation (-45±5 mV) and less stable after irradiation (-14±3 mV). The apparent aggregation might be due to this low zeta value at pH 7.0. In addition, the resulting shape may be due to the templating action of CTAB during reaction of the Te and Pt at high temperature.In order to accelerate the circulation of NPs in the bloodstream, their size must be in the range of 50 nm to avoid the clearance by reticulo-endothelial systems such as liver, spleen and kidneys[39]. Another important feature of the TePt NWrs was found to be high crystallinity as shown SAED pattern in (Fig.2e). Crystalline materials are found to have very high thermal conductivity, an important asset for agents used in PTT[40]. X-ray diffraction (Fig. 2f) of the TePt NWrs was characterized based on the data from Joint Committee on Powder Diffraction Standards and previous findings by other researchers[37]. As per the given standards in terms of peaks, the TePt was found to have rhombohedral phase of Pt_3Te_4. The elemental composition in the form of EDAX of TePt is presented in Figure 2g. It shows presence of both the element having Pt: Te ratio approximately 3:4.36 which corresponds to Pt_3Te_4, thus confirming the results of XRD. The advantage of Pt_3Te_4 over other phases of Te and Pt chalcogenides (TePt, $TePt_2$, and Pt_2Te_3) is its exceptional thermodynamic stability, which can be exploited, in the

present context for photothermal stability under the physiological condition. Pt_3Te_4 is formed from Pt_2Te_3 during temperature-induced transformation of former one.

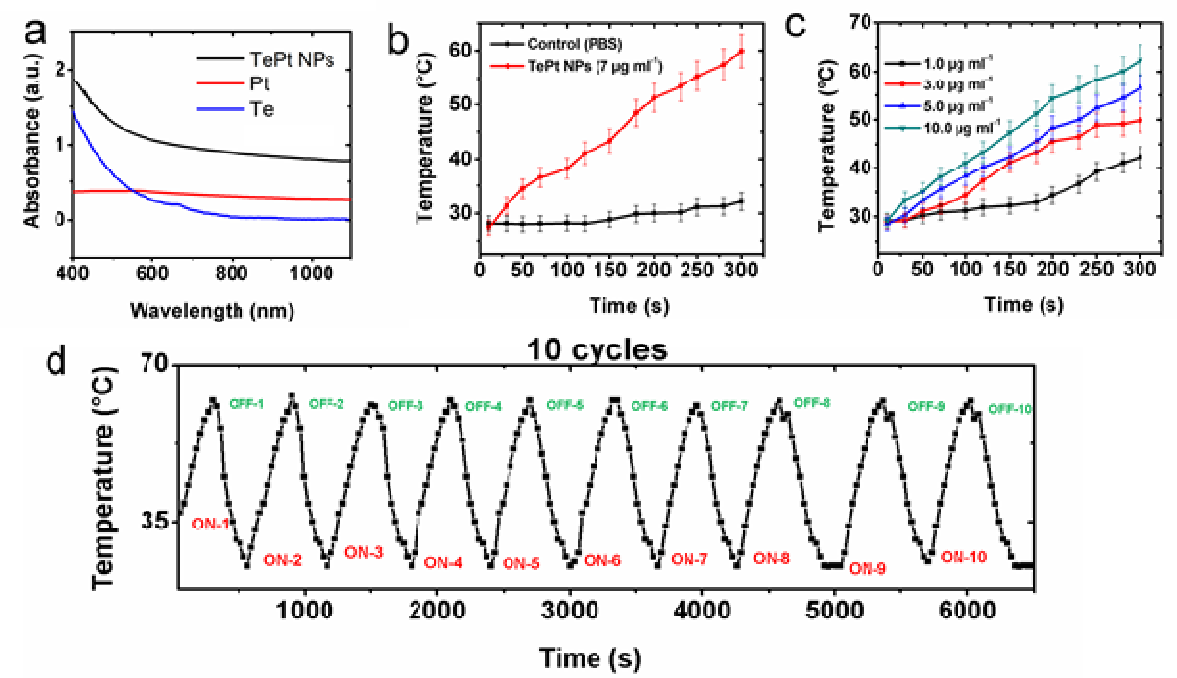

Figure 3. Optical and thermal properties of TePt NWrs (a) UV-Vis-NIR spectra, (b) temperature enhancement with respect to time (c) Concentration dependent temperature enhancement and (d) thermal stability curve after 10 cycles of ON-OFF till 6000 seconds.

Figure 3a displays the UV-Vis-NIR spectra of tellurium nanowires and its final growth to TePt NWrs. Tellurium nanowire exhibited signature absorbance at around 680 nm due to due to electronic transition from P-lone pair valance bond to the P-anti-bonding conduction band, due to semiconducting nature of tellurium[41-43]. After reaction with Platinum salt, there were two cardinal observations, first, the signature absorbance of tellurium nano-wires got vanished and second, the absorbance of TePt NWrs was enhanced to a great extent. This optical change in the structure is in the favor of photothermal energy since it will enhance the photothermal efficiency of the nano-conjugate. The absorbance of TePt NWrs in NIR regime (1000 nm and up) is helpful in one of the most potential cancer therapy called photothermal therapy. This region is

considered to be most significant for biological applications due to its high penetrability inside the body as well as least absorption by blood and other biological fluids[38].

The enhancement of temperature with respect to time is shown in Fig. 3b. After irradiation of the laser (NdYAG, 808 nm, 1 W/cm^2), for 10-12 min, TePt NWrs exhibited high heat enhancement capacity. The temperature of TePt NWrs was found to increase to 60±2°C from room temperature, a total increment of ~35°C. The temperature of the phosphate buffered saline as control was found to enhance to 34°C.

In order to tune the optimum amount of TePt NWrs for temperature enhancement, different amount of TePt NWrs (1-10 μg/ml) was taken in PBS and irradiated with laser for 15 min (Fig. 2c). After the careful scrutiny, 10 μg/ml aqueous suspension of TePt NWrs was found to have maximum influence on the enhancement of temperature with respect to control, as shown in the Fig. 3b, c. After the exposure of laser (1 W/cm^2), the temperature was raised to 60°C as shown in the Fig. 3c.

In order to assess the thermal stability of the TePt NWrs, nearly 10 μg/ml of the sample was taken in a micro-cuvette and irradiated with the NdYAG laser for 200 seconds and allowed to cool for the same time. The process was repeated 10 times and represented graphically (Fig. 3d). The heating and cooling profile of the TePt NWrs was found to be uniform throughout the cycle thus proving its relevance for the photothermal therapy. This is an important attribute of the nanoparticle, which are appreciated as an ideal candidate for photothermal therapy to have capacity to withstand the exposure of intense laser. The power of the laser was adjusted to 1±0.5 W/cm^2 and the exposure area was adjusted to 3-4 mm to reduce the unwanted exhaustion of the laser power. In variety of photothermal therapies, the power of the laser was adjusted to >10 W/cm^2 to achieve sufficiently high killing rate of the cancer cells[39]. The lacunae of such high laser intensity are destruction of the normal tissue of the cells such as intestinal linings as it is far beyond the recommended intensity for exposure to human skin 0.35±2 W/cm^2.

Photothermal transduction efficiency (PTE) of the TePt NWrs were calculated using methods described elsewhere[38] (Li et al. 2014). Following equation was used to calculate the PTE of the NPs:

$$\eta = \frac{hs(T_{\max} - T_{Out}) - Q_{in,0ut}}{I(1-10^{-A_{808\,nm}})} \qquad (2)$$

Where *hs* is the product of heat transfer coefficient and surface area of the cuvette, T_{max}-T_{out} is the difference between the heat of system and surrounding after exposure of 10 µg/ml of TePt NWrs for 10 min, A_{808nm} is the intensity of absorption at 808 nm and $Q_{in,\,out}$ is the dissipation of the heat by solvent and container. The details of the calculations are presented in Supporting information. The PTE was found to be 42.7%, which is much higher than many nano-composites such as gold NRs (22±1%, 808 nm laser), CuSe (22%, 980 nm laser), and CuS (25.7%, 980 nm laser)[44] (Tian et al. 2011).

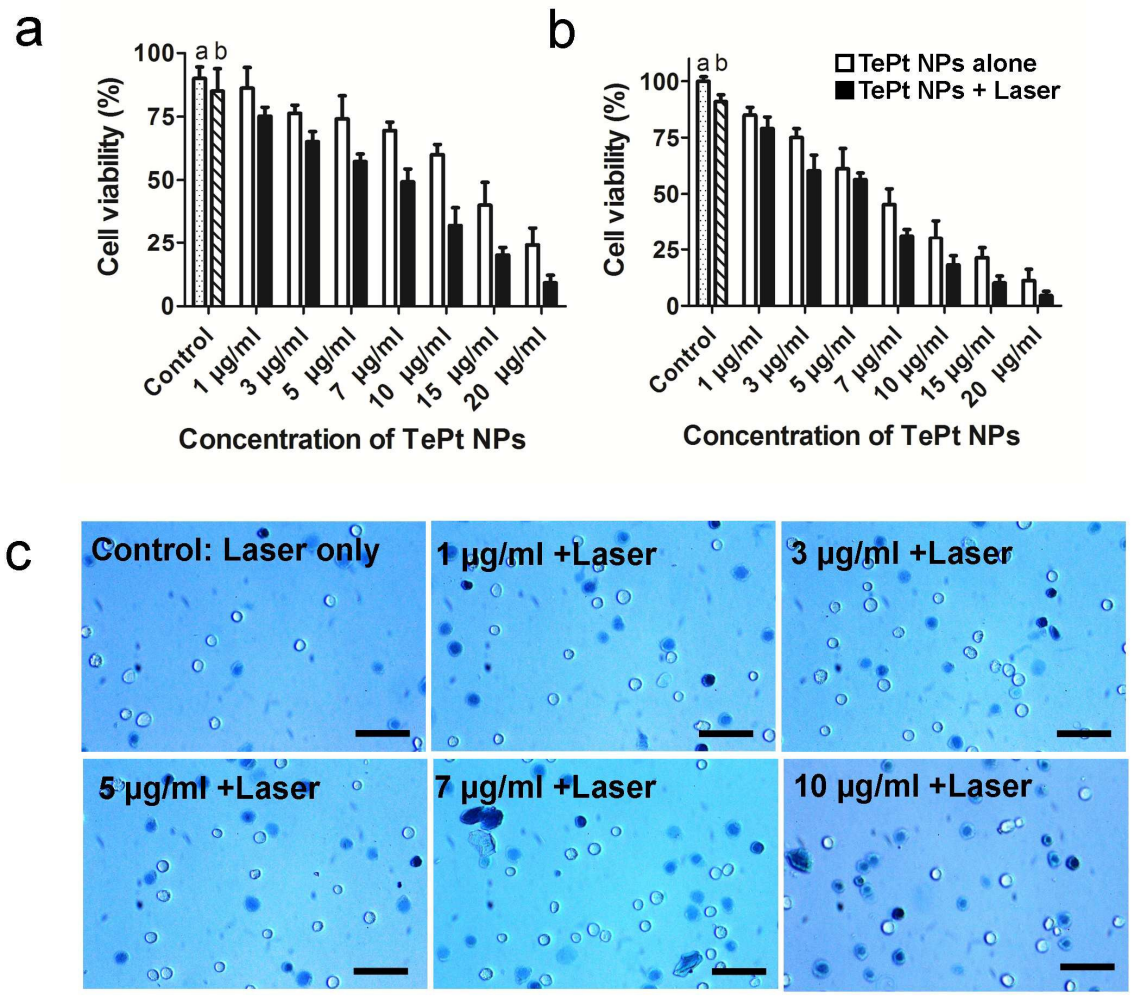

Figure 4. Cytotoxicity analysis of the NPs on A549 cells using (a) Trypan blue (b) MTT assay (Control 'a' is cells only and Control 'b' cells plus laser only) and (C) the impact of laser irradiation on the viability of cells is explained with respect to concentration of TePt NWrs using trypan blue (0.4 % in PBS, pH 7). Scale bar represents 100 µm.

Comprehension of biocompatibility of NPs under biological consideration becomes mandatory in order to prove the efficacy for the proposed cancer therapy. The toxicity of the TePt NWrs was assessed on A549 cells using trypan blue and MTT assay with and without exposure to laser (Fig. 4a, b). There was substantial depletion of cell survival after the exposure of laser (808 nm, 0.1 W/cm^2) for 300 s (Total energy 30 Joules). At optimum concentration of TePt NWrs (10 µg/ml), the survival of the cells was found to be nearly 25% in comparison to ~68% without

exposure to laser for 5 min as depicted in the Fig. 4a, b. At higher concentration, till 20 µg/ml, the viability drops down to 9 % and 5 % as given by trypan blue and MTT assay, showing almost complete abrogation of cancer cells. The lower panel of Fig. 4 displays viability of the A549 cells using Trypan blue (0.4%, pH 7.0). Live and dead cells were determined on the basis of the color of the cells after incubation with trypan blue for 5-7 min. As shown in the Fig 4c, the impact of concentration of TePt NWrs was found to significant. With respect to control (not exposed to laser light), the number of cells death was found to increased proportionately with the concentration of the TePt NWrs. Number of blue cells (dead cells due to uptake of the dye) was found to be increased with respect to concentration, thus explaining the inimical effect of laser induced heat on the A549 cells.

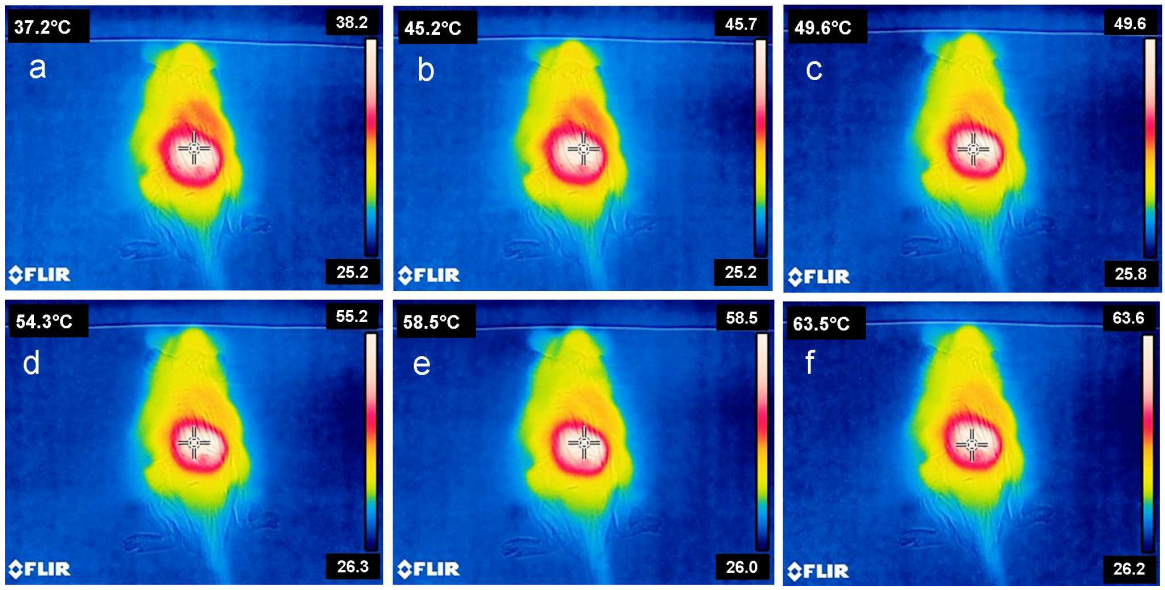

Figure 5. The enhancement in the tumor temperature upon irradiation of the laser with respect to time (Label a-f as 0, 2, 3, 5,7,10 min respectively). The images were taken using FLIR thermal imaging camera.

Figure 5 explains the impact of laser irradiation on the temperature enhancement of tumor after injection of the TePt NWrs in the tumorous regime. The temperature of the tumor was found to

be enhanced form 37°C to 63.6°C after exposure of the laser for 10 min. This in vivo analysis of hyperthermia proves the efficacy of the NPs in photothermal therapy of the cancer.

The white light image of mice bearing tumor is explained in Figure 6. During the treatment, the tumor size with respect to time was also studied and the result is graphically expressed in Figure 6. After the initial treatment of 18 days in presence of the TePt NWrs as show in Fig. 6a (Upper panel), the tumor volume was reduced from 200 mm^3 to ~ 95 mm^3. This explains the efficacy of the proposed NPs for the cancer therapy. The graphical presentation of changes in tumor volume with respect to time of treatment is presented in Figure 6b. The results are also compared with control using saline injection to the mice for similar tenure as shown in the Figure 6a. The tumor volume (in case of control) was increased to a great extent.

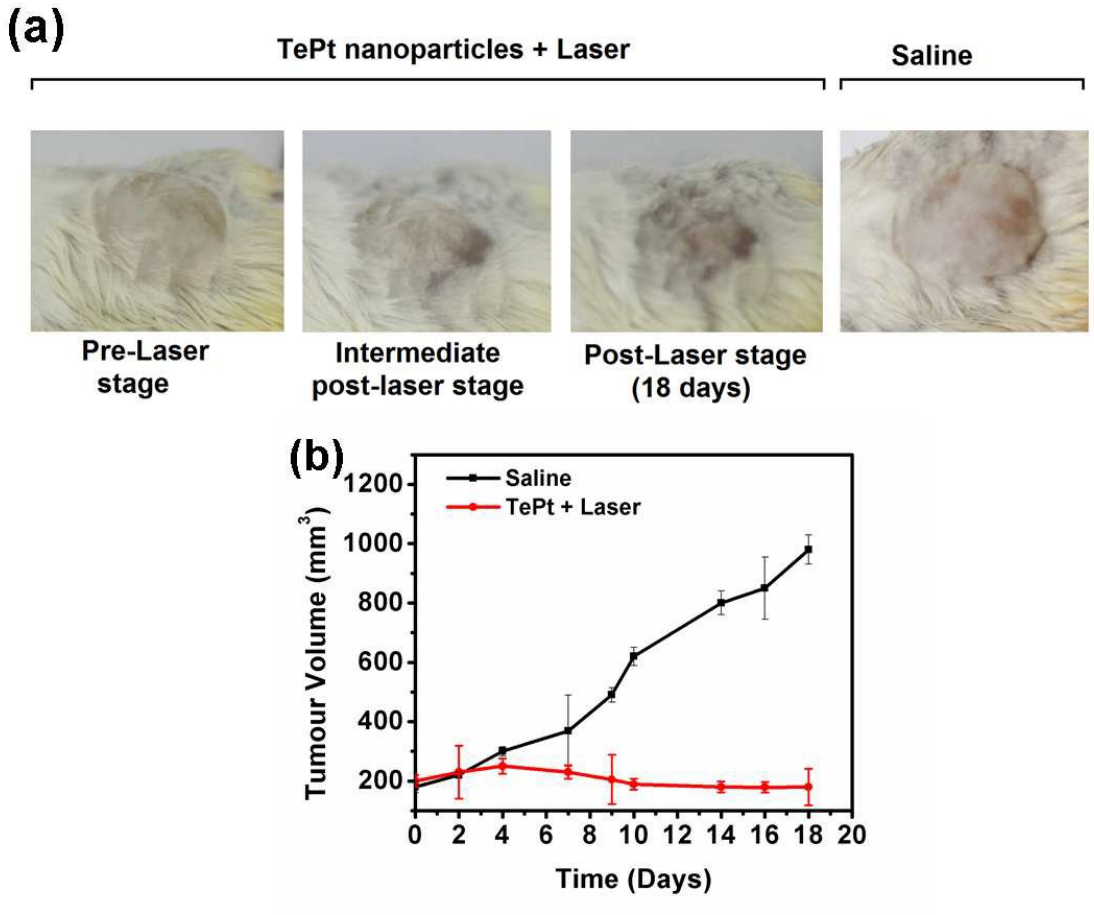

Figure 6. Anti-tumor photothermal activity of TePt NWrs on tumors. (a) Showing tumor images of TePt NWrs injected at pre-laser stage, followed by irradiation (0.5 W/cm^2, 10 min) and intermediate stage after 10 days and post-laser stage after 18 days showing complete destruction of tumour (Black burn marks could be seen due to laser). (b) Showing tumor volume change with respect to time upon nanoparticle treatment and laser irradiation. Saline was used as positive control and was not irradiated. Data is represented as mean± standard deviation (n=5).

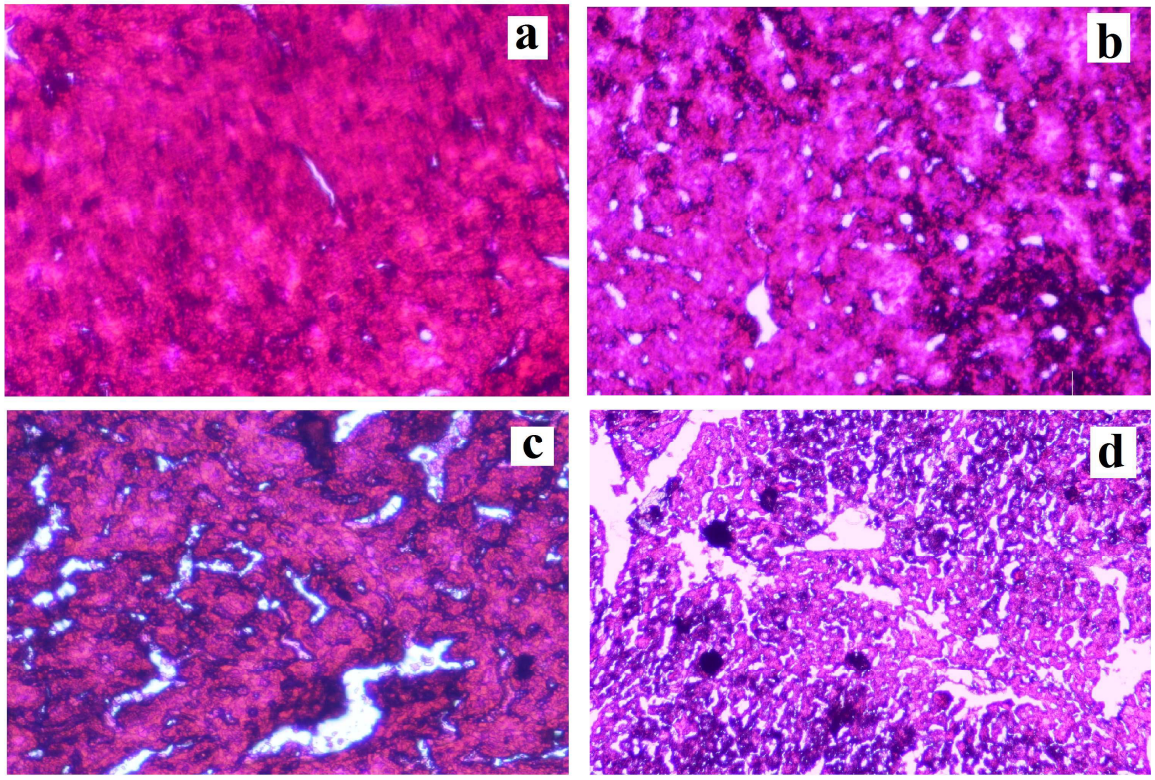

Figure 7. H&E staining of tissue sections of tumors before (a) and after the exposure of laser for (b) 3 (c) 6 and (d) 6 min.

In order to check the microanatomy of the tumor after photothermal therapy, the thin slices of tumor obtained by wax embedding technique was subjected to Hematoxylene and eosin staining and observed under light microscopy (Fig. 7). With respect to control (untreated tumors), there was significant damage observed after increasing the time of exposure of laser from 3 min to 9 min. The mode of cancer cells ablation by TePt NWrs is demonstrated by staining the treated cells PI-Annexin V-FITC conjugate using FACS (Fig. 8). The results were interpreted with respect to control cells (Fig. 8a, without any treatment). The cells were found to be healthy (~99% survival). After the treatment with 10µg/ml TePt NWrs (Fig. 8b), the cells were found to be killed manly by the process of necrosis (PI +ve, Q1). Only 21.24% cells were found to undergo necrosis in the above case. This explains the biocompatibility of the NPs under physiological milieu.

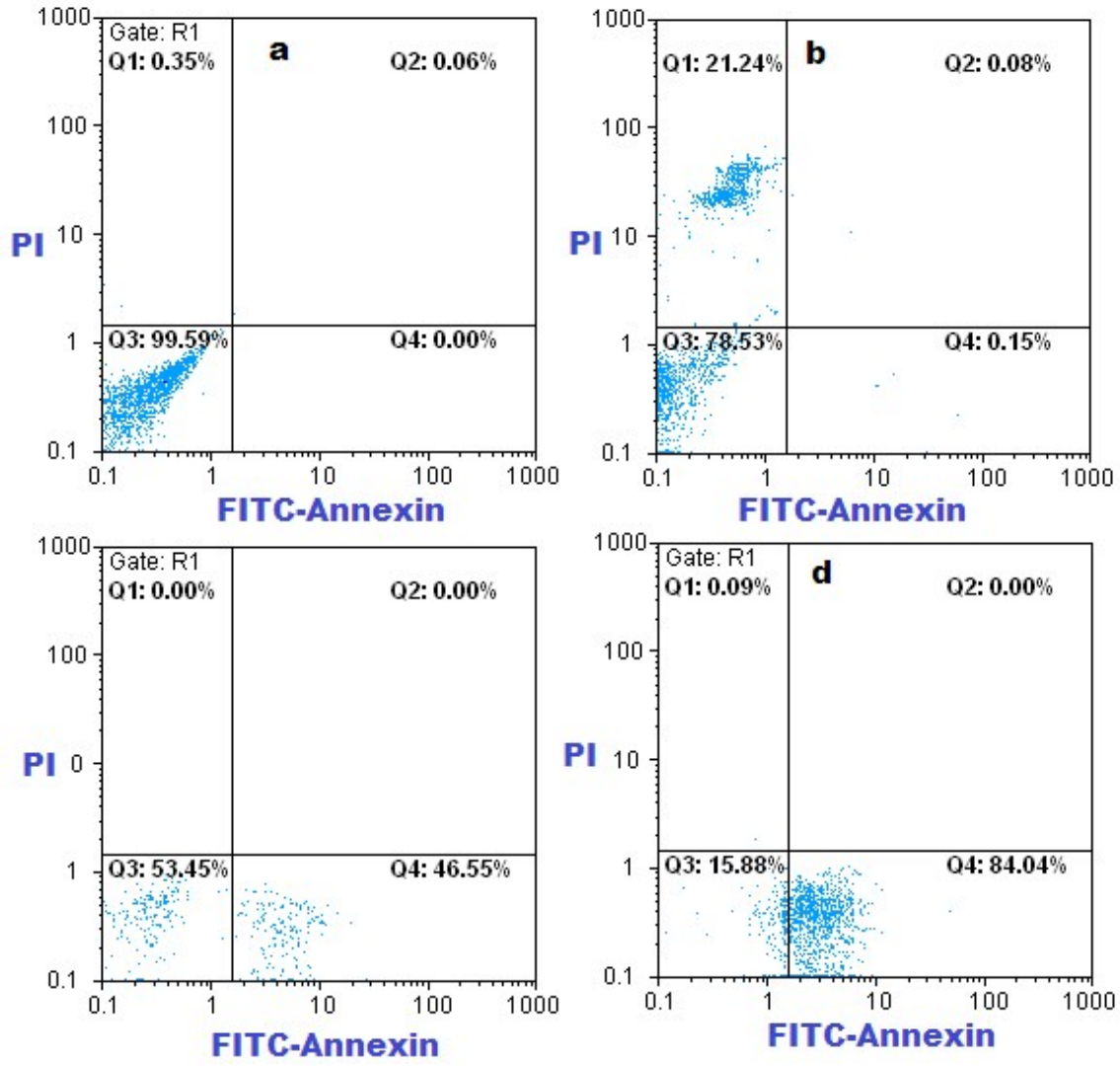

Figure 8. The *modus operandi* of photothermal killing of TePt NWrs via apoptosis determined by FACS using PI-FITC-Annexin V staining (a) A549 cells as a control (b) Cells incubated in with 10µg/ml TePt NWrs without exposure to laser, and (c) cells exposed to 808 nm laser in absence of the NPs (d) Cells with TePt exposed to laser.

Impact of Laser (Fig. 8c, 808nm, 1 W/cm^2) was found to negligible on the cells. Cells were found to be killed by the process of apoptosis (Annexin-FITC +ve, Q4) and necrosis. Figure 8d displays the effect of laser in presence of TePt NWrs. The mode cell death was confirmed to be mainly by apoptosis. ~84% cells were found to by ablate by the process of apoptosis thus verifying the mode of cell death.

4. Conclusions

The platinum chalcogenides called tellurium Platinate (Pt_3Te_4) was found to be exceptionally important for photothermal therapy of Cancer cells, mainly due to the semiconducting property of tellurium. The high photothermal conversion efficiency of the nano-conjugate catalyzed the enhancement of ~ 35°C from room temperature. The tumor size was found to deceased be with respect to time after the exposure of laser in presence of nano-conjugate. Alteration in the internal anatomy was studied by H&E staining of thin slices made by microtomy. In sum, the impact of photothermal property was found to be pivotal in in vitro as well as in vivo studies.

References

1. R. Jain, *Advanced drug delivery reviews*, 2012, **64**, 353-365.
2. P.Vinod, U. Siddik, G.Viswanathan, G. Chandrasekharan, NPs in drug delivery and cancer therapy: the giant rats tail. *Journal of Cancer Therapy*, 2011, **2**, 325-334
3. A. Gormley, N. Larson, A. Banisadr, R. Robinson, N. Frazier, A. Ray, H. Ghandehari, *J. Controlled Release*, 2013, **166**,130-138.
4. M. Konerdingi, E.Fait, A.Gaumann, C. Dimitropouloui,W. Malkusch, *Angiogenesis: Models, Modulators, and Clinical Applications, Plenum Press, New York, USA*, 429-447.
5. Jain, R.K., *Cancer research*, 1987, **47**, 3039-3051.
6. L.Baxter, R.Jain, *Microvascular research*, 1989, **37**, 77-104.
7. C.E.Probst, P.Zrazhevskiy, V. Bagalkot, X.Gao, *Advanced drug delivery reviews*, 2013, **65**,703-718.
8. K.Fujiwara, T.Watanabe, *Pathology International*, 1990, **40**, 79-84.
9. M .S. Khan, H. Abdelhamid, H.-F. Wu. *Colloids and Surfaces B: Biointerfaces,2015* 127281–291.
10. M S. Khan, M. L Bhaisare, H.F. Wu. *Journal of Industrial and engg chemistry*. doi:10.1016/j.jiec.2015.12.011
11. Z. Lin, , Z.Yang, H. Chang, *Crystal Growth and Design,* 2007, **8**, 351-357.

12. C.W. Song, *Cancer Research*, 1984, 44(10 Supplement), 4721s-4730s.

13. H. Wang, L. Chen, Y. Feng, H. Chen, *Accounts of chemical research*, 2013, **46**, 1636-1646.

14. H.Yuan, A. Fales, T. Dinh, *J. Am. Chem. Soc.*, 2012, **134**, 11358-11361.

15. M.Gellner, D.Steinigeweg, S.Ichilmann, M.Salehi, M.Schütz, K.Kömpe, M.Haase, S.Schlücker, *Small*, 2011,**7**, 3445-3451.

16. J. Wang, W. W. Zhao, H. Zhou, J. J. Xu, H. Y. Chen. *Biosensors and Bioelectronics*, 2013, 41, 615–620

17. S. Pandey, M. Thakur, A. Mewada, D.Anjarlekar, N.Mishra, M.Sharon, *J. of Materials Chem B*, 2013, **1**, 4972-4982.

18. C.M.Hessel, V.Pattani, M. Rasch, M.Panthani, B.Koo, J.Tunnell, B. Korgel, *Nano letters*, 2011, **11**, 2560-2566.

19. S.B C.M.Hessel, V.Pattani, M. Rasch, M.Panthani, B.Koo, J.Tunnell, B. Korgel, *Nano letters*, 2011, **11**, 2560-2566.

20. Y.Huang, X. Duan, Y.Cui, L. Lauhon, K. Kim, C. Lieber, *Science*, 2001, **294**, 1313-1317.

21. C. Murray, C. Kagan, M. Bawendi, *Science*, 1995, **270**, 1335-1338

22. Y. Xia, P.Yang, Y.Sun, Y.Wu, B.Mayers, B.Gates, Y.Yin, F.Kim, H. Yan, *Advanced materials*, 2003, **15**, 353-389.

23. Batabyal, J.Vittal, *Chemistry of Materials,* 2008, **20**, 5845-5850.

24. N. Gaponik, D. Talapin, A. Rogach, A. Eychmüller, *J. Mater. Chem.*, 2000, **10**, 2163-2166.

25. S.Günes, H.Neugebauer, N. Sariciftci, J.Roither, M.Kovalenko, G.Pillwein, W.Heiss, *Advanced Functional Materials*, 2006, **16**, 1095-1099.

26. Y.Li, H. Zhong, R.Li, Y.Zhou, C.Yang, Y. Li, *Advanced Functional Materials*, 2006, **16**,1705-1716.

27. R.Venkatasubramanian, E.Siivola, T.Colpitts, B.O'quinn, *Nature*, 2001, **413**, 597-602.

28. S Mamedova, N.A. Kotov, A. Rogach, J.Studer,. *Nano Letters*, 2001, **1**, 281-286.

29. N. Mingo, *Applied physics letters*, 2004, **85**, 5986-5988.

30. P. Norton, *Optoelectronics review,* 2002, **3**, 159-174.

31. .Wang, N. Mamedova, N.A. Kotov, W. Chen, J.Studer, *Nano letters*, 2002, **2**, 817-822.

32. Q.Yan, H.Chen, W. Zhou, H. Hng, F. Boey, J. Ma, *Chemistry of Materials*, 2008, **20**, 6298-6300.

33. H. Zhong, Y.Zhou, Y.Yang, C.Yang, Y.Li,. *J. Phys. Chem. C*, 2007 , **111**, 6538-6543.

34. D. Cobden, *Nature*, 2001, **409**, 32-33.

35. Y.Cui, Q.Wei, H.Park, C. Lieber, *Science*, 2001, **293**, 1289-1292.

36. G. Prinz, *Science*, 1998, **282**, 1660-1663.

37. A. Samal, T. Pradeep, *Langmuir*, 2010, **26**, 19136-19141.

38. Z. Liu, L. Cheng, L. Zhang, Z. Yang, Z. Liu, J. Fang, *Biomaterials*, 2014, **35**, 4099-4107

39. X.-Dong, Z. Jie, C. Jiang, Y. J. -Ying, W. Xiu, S. S.-Sha, S. Hao, W. Hua, H. X. Wang , S. Fan, Y-M. Sun, M. Guo, *J. Mater. Chem. B*, 2015, **3**, 4735-4741

40. L.Gu, A. Koymen, S. Mohanty, *Scientific Reports,* 2014, **4**, 5106.

41. U. Gautam, C.Rao, *J. Mater. Chem.* **14**, 2530-2535.

42. A.Jain, A.Agarwal, S.Majumder, N.Lariya, A. Khaya, H. Agrawal, S. Majumdar, G. Agrawal, *J. Controlled Release*, 2010,**3**, 359-367.

43. T. Sreeprasad, A. Samal, T. Pradeep, *J. Phys. Chem. C*, 2009, **113**, 1727-1737.

44. B.Li, F.Fu, K.Xu, R.Zou, Q.Wang, B. Zhang, Z.Chen, J.Hu, Facile Synthesis of Biocompatible Cysteine-coated CuS NPs with High Photothermal Conversion Efficiency for Cancer Therapy. Dalton Transactions. 2014, **43**, 11709-11715